doi:10.1111/j.1558-5646.2011.01538.x

CONCERTED VERSUS INDEPENDENT EVOLUTION AND THE SEARCH FOR MULTIPLE REFUGIA: COMPARATIVE PHYLOGEOGRAPHY OF FOUR FOREST BEETLES

Katharine A. Marske,[1,2,3,4] Richard A. B. Leschen,[1] and Thomas R. Buckley,[1,2,5]

[1]*Landcare Research, Private Bag 92170, Auckland 1142, New Zealand*

[2]*School of Biological Sciences, University of Auckland, Private Bag 92019, Auckland 1142, New Zealand*

[3]*Center for Macroecology, Evolution and Climate, University of Copenhagen, Universitetsparken 15, DK-2100 Copenhagen Ø, Denmark*

[4]*E-mail: kamarske@bio.ku.dk*

[5]*Allan Wilson Centre for Molecular Ecology and Evolution, New Zealand*

Received August 20, 2011
Accepted December 1, 2011
Data Archived: Dryad doi:10.5061/dryad.54nq349m

Phylogeographic structure and its underlying causes are not necessarily shared among community members, with important implications for using individual organisms as indicators for ecosystem evolution, such as the identification of forest refugia. We used mitochondrial DNA (cox1), Bayesian coalescent ancestral state reconstruction (implemented in BEAST), and ecological niche models (ENMs) to construct geospatial histories for four codistributed New Zealand forest beetles (Leiodidae, Nitidulidae, Staphylinidae, and Zopheridae) to examine the extent to which they have tracked environmental changes together through time. Hindcast ENMs identified potential forest refugia during the Last Glacial Maximum, whereas ancestral state reconstruction identified key geographic connections for each species, facilitating direct comparison of dispersal patterns supported by the data and the time frame in which they occurred. Well-supported geographic state transitions for each species were mostly between neighboring regions, favoring a historical scenario of stepping stone colonization of newly suitable habitat rather than long distance dispersal. No geographic state transitions were shared by all four species, but three shared multiple projected South Island refugia and recent dispersal from the southernmost refugium. In contrast, strongly supported dispersal patterns in the refugia-rich northern South Island suggest more individualistic responses to environmental change in these ecologically similar forest species.

KEY WORDS: Ancestral state reconstruction, *Brachynopus scutellaris*, coalescent phylogeography, *Hisparonia hystrix*, New Zealand, *Nothofagus* gap.

Comparative phylogeography seeks to understand ecosystem evolution by identifying shared responses to historical events among disparate taxa (Bermingham and Moritz 1998). The late-Pleistocene Last Glacial Maximum (LGM), which had a major influence on the past and present distributions of the global biota, has been a particular focus of comparative phylogeographic studies (Waltari et al. 2007). Although "classical" patterns of species response to Pleistocene climate change have been identified, such as the "southern richness, northern purity" distribution of genetic diversity in Europe (Hewitt 2000), a growing body of data on

codistributed taxa indicate that phylogeographic structure and its underlying drivers are not necessarily shared among community members (e.g., Soltis et al. 2006), with important implications for using individual organisms as indicators for ecosystem persistence (e.g., forest refugia). Sullivan et al. (2000) found that species with qualitatively similar phylogenies shifted neither in concert nor as differently as expected under independent responses to climate change (here "concerted evolution" refers to shared phylogeographic histories in different species, after Sullivan et al. (2000), rather than genetic evolution within a species), whereas Carstens et al. (2005) observed that looking for genetic concordance among codistributed species assumes they were codistributed in the past, which is rarely tested. Soltis et al. (2006) highlighted the issue of pseudocongruence, in which spatially similar genetic patterns can be generated at different times by different causes.

Subsequent applications of coalescent methods and/or ecological niche models (ENMs) have identified specific instances of cryptic incongruence among species with superficially similar histories: Carstens and Richards (2007) detected similar phylogeographic patterns and modern distributions in species from different ancestral refugia, whereas Leaché et al. (2007) inferred different time scales for vicariance around a "common" phylogeographic barrier. In the marine realm, Ilves et al. (2010) detected different patterns of persistence and colonization in members of the North Atlantic intertidal community, whereas McGovern et al. (2010) found different temporal population histories underlying apparently similar genetic variation in two codistributed species. To understand the biogeography of an ecosystem, not just the individual taxa inhabiting it, these results emphasize the need for rigorous phylogeographic methods, validation of assumptions of ancestral congruence (such as ENMs or fossils), and comparative studies across a broad spectrum of available taxa (e.g., Carstens and Richards 2007).

We address the difference between the biogeography of an ecosystem and those of its constituent species. New Zealand is an ideal setting for comparative phylogeography and evolutionary studies because of its turbulent geological history, in which Pleistocene glaciation overlaid 10 million years of significant tectonic reorganization of the landscape and uplift of the major mountain ranges (King 2000; Pulford and Stern 2004). New Zealand experienced montane and valley glaciation, rather than major ice shields (Suggate and Almond 2005), and exposed continental shelf from lowered Pleistocene sea levels may have been more important for glacial refugia than extant terrestrial areas (e.g., Alloway et al. 2007). Evidence for temperate forest refugia in the higher latitudes of the South Island (McGlone 1985; Shepherd et al. 2007; Leschen et al. 2008; Shepherd and Perrie 2011) and in close proximity to glaciers (Marra and Thackray 2010) suggests that latitudinal retreat is inadequate for describing phylogeographic patterns.

We will examine whether four codistributed forest beetles from similar temperate lowland forest microhabitats comprise an "evolutionary cohort", members of a community who track environmental changes together through time (Carstens and Richards 2007), or whether climate change response is more species-specific. Recently developed coalescent phylogeography methods and ENMs will be implemented to identify LGM forest refugia and patterns of gene flow utilized by each species. Assuming similar LGM refugia among species, three scenarios are possible: (1) if temporal and spatial patterns of colonization concur, species likely moved through the Pleistocene together as a semi-intact community; (2) similar spatial patterns but different time scales suggest an intermediate scenario, in which glaciation or older processes may drive superficially similar patterns; and (3) different spatial patterns suggest separate evolutionary trajectories in response to Pleistocene climate change. Each scenario has distinct implications for understanding community formation and temporal stability, and how ecosystems are likely to respond to future climate change.

Methods

SAMPLING

Focal taxa include *Agyrtodes labralis* (Broun) (Leiodidae), *Brachynopus scutellaris* (Redtenbacher) (Staphylinidae), and *Epistranus lawsoni* (Sharp) (Zopheridae), which feed on fungi in dead wood and leaf litter, but are not limited to a specific wood type and are widely distributed in New Zealand forests, making them useful indicator species of any native forest established long enough to generate woody debris (Löbl and Leschen 2003; Marske et al. 2009; Marske et al. 2011). *Hisparonia hystrix* (Sharp) (Nitidulidae) is an arboreal feeder on sooty moulds, which grow primarily on southern beech (*Nothofagus* spp.; Nothofagaceae) and manuka (*Leptospermum scoparium* Forst. & Forst.; Myrtaceae) trees fed upon by honeydew-secreting scale insects (Carlton and Leschen 2007), and is present in scrub, forest margin, and tall forest. *A. labralis* is absent from the North Island (Seago 2009), but *B. scutellaris*, *E. lawsoni* (the only flightless species included), and *H. hystrix* are widely distributed throughout New Zealand, although *B. scutellaris* is absent from the Westland *Nothofagus* gap, an area of the South Island's west coast across which the distribution of *Nothofagus* is disjunct (Leathwick 1998; Leschen et al. 2008). Specimen collection protocols followed Leschen et al. (2008) and Marske et al. (2009, 2011). Geographic information system (GIS) locality information was recorded for each collection site.

ECOLOGICAL NICHE MODELING

ENMs were generated in Maxent 3.3.1 (Phillips et al. 2006; Phillips and Dudík 2008), and were subject to tenfold

Table 1. Genbank accession codes and best-fit models of sequence evolution for each species. For *Epistranus lawsoni*, models were fitted to individual codon positions (1 + 2 and 3).

Taxon	*N*	Genbank accession number	Sequence evolution model	Population growth and molecular clock model
Agyrtodes labralis	189	GU017127-GU017315	GTR+I+Γ	Exponential growth
		JQ245441-JQ245442		Strict clock
Brachynopus scutellaris	340	EU145131-EU145243	GTR+I+Γ	Exponential growth
		JQ266926-JQ267152		Relaxed clock
Epistranus lawsoni	168	JF278627- JF278794	HKY+I+ Γ (1 + 2)	Constant size
			GTR+I+Γ (3)	Relaxed clock
Hisparonia hystrix	308	EU145025-EU145130	K81uf+I+Γ	Exponential growth
		JQ267153-JQ267354		Relaxed clock

cross-validation to ensure consistency of model predictions and ecological variable response among repeated runs. The final geographical projections represent the mean point-wise strength of prediction over 10 model runs applied to modern and LGM environmental layers. Climate variables for current and LGM projections included mean annual rainfall, mean February (summer) rainfall, mean annual solar radiation, mean annual temperature, mean February temperature, minimum temperature of the coldest month, and October (winter) vapor pressure deficit, all at 100-m resolution (Leathwick et al. 1998; Leathwick et al. 2003). LGM (about 22,000 calibrated years ago) projections were based on temperature depression estimates from marine isotope stages and LGM topography estimates from lowering the modern DEM to the 120-m bathymetry (J. R. Leathwick, unpubl. data; see Marske et al. 2009 for details).

Localities for *A. labralis* were the same (91) as in Marske et al. (2009), including DNA specimens plus additional collection records, and results for *E. lawsoni* are reported in Marske et al. (2011) based on 173 localities. For *B. scutellaris* and *H. hystrix*, which were subject to focused sampling over multiple years (e.g., Leschen et al. 2008), localities for DNA specimens were visually "thinned" in ArcGIS ver. 9.2 (Environmental Systems Research Institute, Redlands, CA), so that the resulting localities (139 and 134, respectively), were separated by at least 5 km. This was to reduce spatial autocorrelation from sampling some sites multiple times, obtaining a slightly different GIS reading each time. Maps of input localities are shown in Figure S1.

Model performance was evaluated using the threshold-dependent binomial omission tests and the Area Under the (Receiver Operating Characteristic; ROC) Curve (AUC) calculated by Maxent; AUCs > 0.75 are typically considered adequate for species distribution modeling applications (Pearce and Ferrier, 2000). To ensure that significant AUCs represented true difference from random, rather than collection bias (e.g., sampling only from native forests; Raes and ter Steege 2007), and due to concerns over whether subdividing the data for training and testing, as above, constitutes a statistically independent test (Phillips et al. 2009; Veloz 2009), null models were developed to compare our species' model performance against points randomly drawn from areas with native forest cover. For each species, 99 sets of the same number of localities were randomly drawn from areas of native forest (e.g., 99 sets of 173 localities for *E. lawsoni*; see Marske et al. 2011 for details). We modeled all 99 randomly-drawn datasets plus actual data from each target species, without setting aside test data, and ranked the 100 AUCs for each species. Empirical AUCs within the top 5% were considered significantly different from random (after Raes and ter Steege 2007).

The current distributions of *A. labralis, B. scutellaris*, and *E. lawsoni* were also modeled with the addition of three vegetation layers, *Nothofagus* spp., Podocarpaceae, and Myrtaceae (all in stems/hectare), to assess whether beech forest was a strong predictor of the distribution of *B. scutellaris* and, if so, whether this predictive relationship was unique to *B. scutellaris*. Vegetation layers were generated using Generalized Additive Models and survey data from 14,540 forest plots (see Leathwick 2001; Leathwick and Austin 2001 for details).

DNA SEQUENCING AND SEQUENCE STATISTICS

Published mitochondrial DNA sequences were compiled for all species from our previous work (Table 1), and combined with genomic DNA extracted from an additional 2 *A. labralis*, 227 *B. scutellaris*, and 203 *H. hystrix* from the North, South, and Stewart Islands. Total genomic DNA extraction, purification, and sequencing of new specimens followed the protocol in Marske et al. (2009), with the entire specimen ground for digest. The 3′ end of the mtDNA cytochrome oxidase subunit 1 (*cox1*) gene region (approximately 800 base pairs) was amplified using the primers C1-J-2195 and TL2-N-3014 (Simon et al. 1994) under PCR conditions in Leschen et al. (2008) and Marske et al. (2009). Sequences were aligned and edited using BioEdit 7.0.5 (Hall 1999). Tajima's *D* was calculated using DnaSp 5.0 (Rozas et al. 2003) to test for evidence of selection, and was nonsignificant

for all species. The best-fit model of sequence evolution for each species (Table 1) was determined using the Akaiki Information Criterion implemented in Modeltest 3.7 (Posada and Crandall 1998) and PAUP*4.0b10 (Swofford 1998).

COALESCENT PHYLOGENETIC AND MOLECULAR CLOCK ANALYSES

To select appropriate molecular clock and population growth models for coalescent phylogeography implementation (see below), molecular clock analyses were conducted in BEAST 1.5.3 (Drummond and Rambaut 2007) using the sequence evolution models in Table 1. As no external calibration points exist for any of these species, we utilized Papadopoulou et al.'s (2010) Coleoptera mitochondrial sequence divergence rate of 3.54% My^{-1}. Unlike the heavily utilized Brower (1994) rate of 2.3% My^{-1}, which was derived using both protein-coding and ribosomal markers, the rate of 3.54% My^{-1} was estimated specifically for *cox1* under a relaxed clock (Papadopoulou et al. 2010). Markov chain Monte Carlo (MCMC) analyses were performed under both the strict and relaxed (uncorrelated lognormal) clock, under both the constant size and exponential growth population models. We allowed some rate flexibility even under the strict clock model by setting a normal prior distribution for clock rate (mean = 0.0177, SD = 0.00177), rather than a fixed rate. Under the relaxed clock, we used a normal prior for mean rate (mean = 0.0177, SD = 0.00177) and exponential priors for coefficient of variation and covariance (mean = 1.0).

Each BEAST profile ran five times for 50 million generations, logging every 2000 (except *E. lawsoni*, which ran for 20,000, logging every 1000), and log files from each set of runs were combined using LogCombiner (Drummond and Rambaut 2007). To select among clock and population growth models, log files were imported into Tracer 1.5 (Rambaut and Drummond 2009) to assess whether the marginal posterior distribution of Euclidean standard deviation or the growth rate parameter included zero. Tree files were reduced in size and combined (burn-in = 6250, thinning interval = 5000; 2000 and 2000 for *E. lawsoni*) using LogCombiner and TreeAnnotator (Drummond and Rambaut 2007) to yield a Maximum Clade Credibility (MCC) consensus tree for each set of analyses.

COALESCENT PHYLOGEOGRAPHIC RECONSTRUCTION

Coalescent ancestral state estimation in a Bayesian framework provides a probabilistic inference of phylogeography from phylogenetic data by estimating both the location and date of each node while accounting for the stochastic nature of evolution (Lemey et al. 2009). Geographic localities of sampled populations are inferred as character states, and historical dispersal between populations is estimated along the branches of the phylogeny using a continuous-time Markov chain (CTMC), which estimates discrete states as a continuous function of time (Lemey et al. 2009). For k localities, $k(k-1)$ geographic state transitions (dispersal patterns) are possible, most of which are unrealistic in nature (e.g., the rate at which geographic state transitions directly connect the northernmost North Island with Stewart Island is most likely zero). To identify the optimal subset of geographic state transitions which explain the data, Bayesian stochastic search variable selection (BSSVS) assigns a binary indicator variable to each geographic state transition parameter, imposing a prior probability of zero on all possible transitions (Lemey et al. 2009; Lohse et al. 2011). This allows a more efficient exploration of MCMC space, identifying both well-supported historical dispersal events and geographic state transitions with a probability of zero (Lemey et al. 2009). Results are a posterior probability estimate for each possible geographic state for each node of the resulting MCC tree. Bayes factors (BF) can then be implemented to identify well-supported nonzero BSSVS parameters; in practice, this identifies geographic state transitions with strong posterior support, typically a subset of all geographic state transitions identified in the phylogeny. In a comparative phylogeography setting, well-supported geographic state transitions can be compared among species to detect whether similar dispersal patterns characterize their phylogeographic histories. Well-supported transitions shared by multiple species can be investigated further, although differences are immediately apparent.

Ancestral state reconstruction was conducted in BEAST 1.5.3 using the relaxed clock and population growth models determined above. Following Lemey et al. (2009), we imposed exponential and gamma priors on the CTMC process and a truncated Poisson prior on the number of nonzero rates. We did not impose (geographic) distance-informed priors because of the complex topography within and between regions; dispersal routes are estimated solely by the genealogical process. Each profile ran five times for 50 million generations, logging every 2000 (except for *B. scutellaris* and *H. hystrix*, which ran for 60 million), and replicate tree files were examined for convergence and combined as above to generate a MCC consensus tree for each species, except for *B. scutellaris* and *H. hystrix*, for which individual tree files were reduced (burn-in = 7500, thinning interval = 5000) and then combined (thinning interval = 4000) due to file size. Discrete rate matrices from all five runs were combined (burnin as above), and the BF test (script available at BEAST website) was applied to the nonzero rates, with BF > 3.0 indicating well-supported geographic state transitions.

To define geographic states for the coalescent analysis, we pooled locality data for *A. labralis*, *B. scutellaris*, and *E. lawsoni* and generated ENMs for the species assemblage using the

methods previously described for individual species. As those methods failed to yield ENMs for *H. hystrix* (see Results), localities for that species were excluded from the pooled dataset. We set a threshold for climatic suitability of ≥0.2, which was near the average lowest prediction for a test locality among the ENM pooled-dataset runs (after Pearson et al. 2007; McCormack et al. 2010). Because modeled refugia include areas no longer above sea level (see Results and Fig. 1), geographic state boundaries encompass all land areas contiguous to the refugia under the assumption that the nearest extant populations will most closely reflect the refugial haplogroups (see Fig. 5 for details). Boundaries are also consistent with mountain barriers for many regions. We used the same geographic states in the coalescent analysis for *H. hystrix* to facilitate comparison of results.

Results

ENMS

Models of the distributions of *A. labralis* and *B. scutellaris* were significantly better than random in binomial omission, ROC, and null model tests. For *A. labralis*, cross-validation runs yielded an average AUC of 0.868 (SD = 0.042, range = 0.803–0.927) and performed significantly better than random at all but the lowest threshold for all runs. Very little "clamping" was detected during LGM projection—this is where environmental conditions in the projection (LGM) climate data exceed those on which the model was trained (e.g., colder temperatures, less precipitation). Maxent treats conditions in these areas the same as the closest observed values (e.g., if training temperatures range from 10 to 20°C, a pixel with LGM temperature of 8°C will be treated the same as one of 10°C) (Anderson and Raza 2010). In the null model test, the AUC for *A. labralis* (0.910) ranked higher than all models for random forest localities (AUC range = 0.844–0.904). For *B. scutellaris,* cross-validation runs yielded an average AUC of 0.831 (SD = 0.079, range = 0.7255–0.9057) and performed significantly better than random across most thresholds and runs. Clamping during LGM projection was restricted to high-elevation areas where the species is absent. In the null model test, *B. scutellaris* (AUC 0.885) ranked higher than models for random forest localities (AUC range = 0.820–0.878).

Projected modern distributions were nearly identical for *A. labralis* and *B. scutellaris* and were broadly congruent to the distribution previously obtained for *E. lawsoni* (see Marske et al. 2011) (Fig. 1). Notably, the central west coast was predicted as highly suitable for all three species, even though *B. scutellaris* is absent there. Adding vegetation layers as predictors reduced suitability for *B. scutellaris* in this area but did not remove Westland from the projected range (Fig. 1B), and *Nothofagus* spp. became the top predictor for the distribution of both *B. scutellaris* (28.5%) and *A. labralis* (27.9%), which is present in the *Nothofagus* gap. Glacial refugia at Karamea and small areas of relatively higher climatic suitability near the Haast River mouth were projected for all three species (Fig. 1). Each species also had a projected refugium between Nelson and Marlborough and/or in Kaikoura; these northeastern refugia were relatively more climatically suitable than those on the west coast.

Models for *H. hystrix* were not significantly better than random. Cross-validation runs yielded an average AUC of 0.758 (SD = 0.042, range = 0.705–0.83), but in the null model test, *H. hystrix* (AUC 0.823) ranked lower than most models for random forest localities (AUC range = 0.822–0.877). Clamping was detected over substantial parts of the South Island during LGM projection, including regions of interest based on the genetic data, indicating model uncertainty in these areas. Therefore, no projections are presented for *H. hystrix*.

PHYLOGENETIC RELATIONSHIPS AND MOLECULAR DIVERGENCE

Root coalescence for *A. labralis* was estimated at 1.95 Ma (95% CI = 1.31–2.61 Ma), roughly 72% as old as that estimated using the Brower (1994) substitution rate (2.69 Ma; Marske et al. 2009). Well-supported regional haplogroups were consistent with those previously identified, including Kaikoura-Marlborough, Nelson, Buller-Canterbury, northern west coast, southern west coast, and southern South Island-Stewart Island (Fig. 2A). Topology was consistent with that previously reported except that the northern west coast comes out as sister to the southern South Island (with low support; posterior probability, hereafter, pp = 0.28), rendering the southern half of the South Island polyphyletic. All clades were allopatric except in the southwestern South Island.

For *B. scutellaris*, root coalescence was estimated at 2.03 Ma (1.31–2.85 Ma), giving rise to four major lineages, although their relationship to each other, with the exception of the root placement, was not well-supported (Fig. 2B). Regional haplogroups are consistent with those identified by Leschen et al. (2008), including eastern South Island, North Island-Brady Creek (Haast River, South Island), and two lineages (A and B, Fig. 2B) which are sympatric through Marlborough and the western South Island. Both A and B straddle the *Nothofagus* gap, although the geographic break was only well-supported in a subclade of B (pp = 0.73), in which lineages north and south of the gap diverged at 0.33 Ma (0.18–0.51 Ma).

An older history was reconstructed for *E. lawsoni*, for which root coalescence was estimated at ∼18 Ma (Fig. 3A; Marske et al. 2011). Clades present in the North Island and northern and eastern South Island were broadly sympatric, whereas all samples from the western and southernmost South Island fell into a single clade also present in the northern North Island. With the exception of one individual from northern Nelson, all South Island lineages within this clade formed a well-supported group (pp = 1),

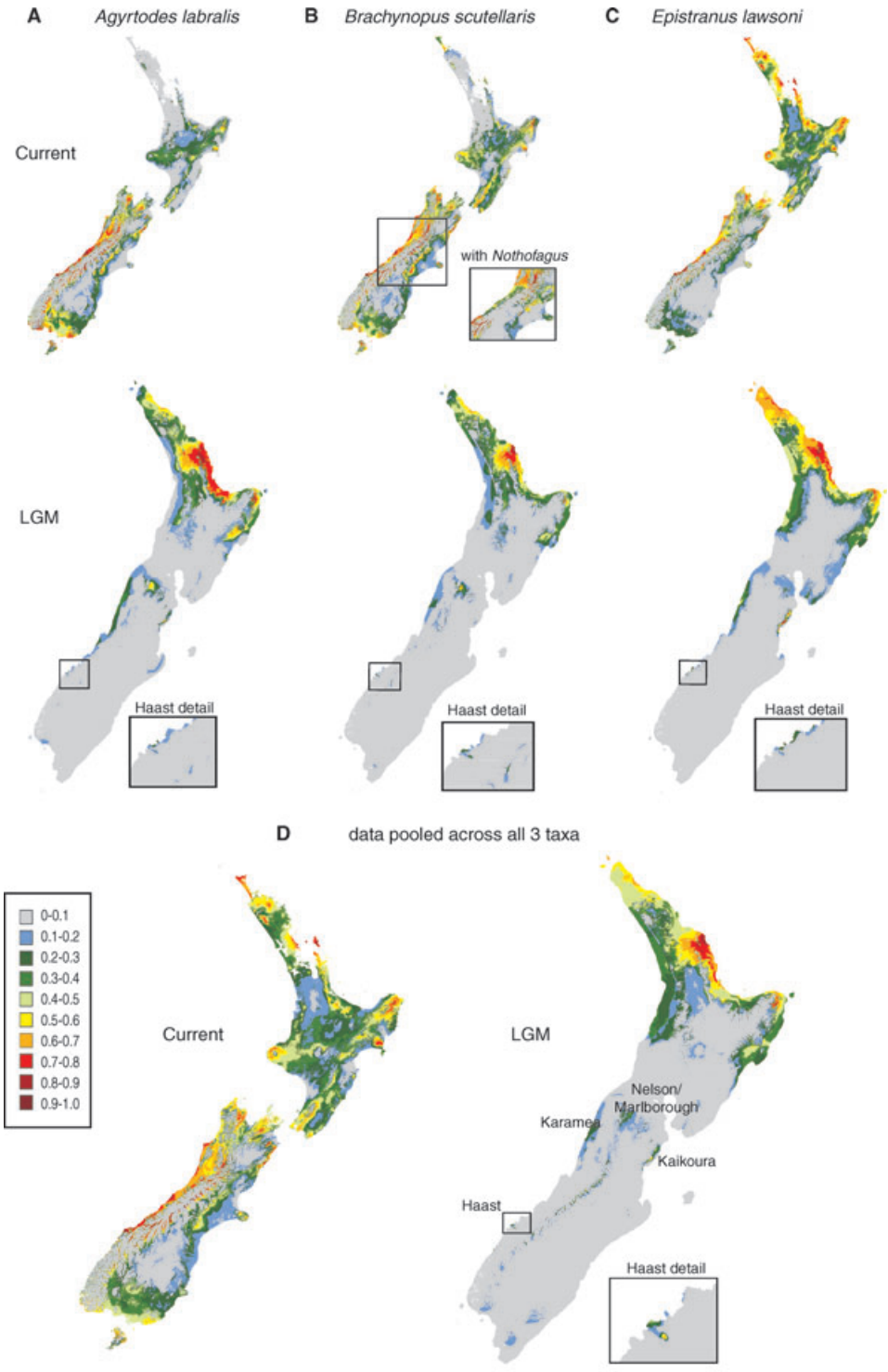

Figure 1. Ecological niche models for (A) *Agyrtodes labralis*, (B) *Brachynopus scutellaris* (C) *Epistranus lawsoni,* and (D) the log-dwelling beetle assemblage, averaged across 10 cross-validation runs, including current and LGM (about 22,000 calibrated years ago) projections and an enlargement of the Haast refugium. Current distributions were modeled with the addition of three vegetation variables, and the central Westland portion of the resulting *B. scutellaris* model is shown (B). Even including *Nothofagus* as a predictor, the projected distribution of *B. scutellaris* includes the *Nothofagus* gap. South Island refugia (labeled in (D)) were shared by at least two of the three species, with the west coast refugia shared by all three, allowing us to test scenarios of concerted versus independent dispersal histories. The LGM projection for the assemblage indicated potentially suitable regions within the Southern Alps, but because these areas were not predicted by any of the single-species models, they were not used to inform the phylogenetic analysis.

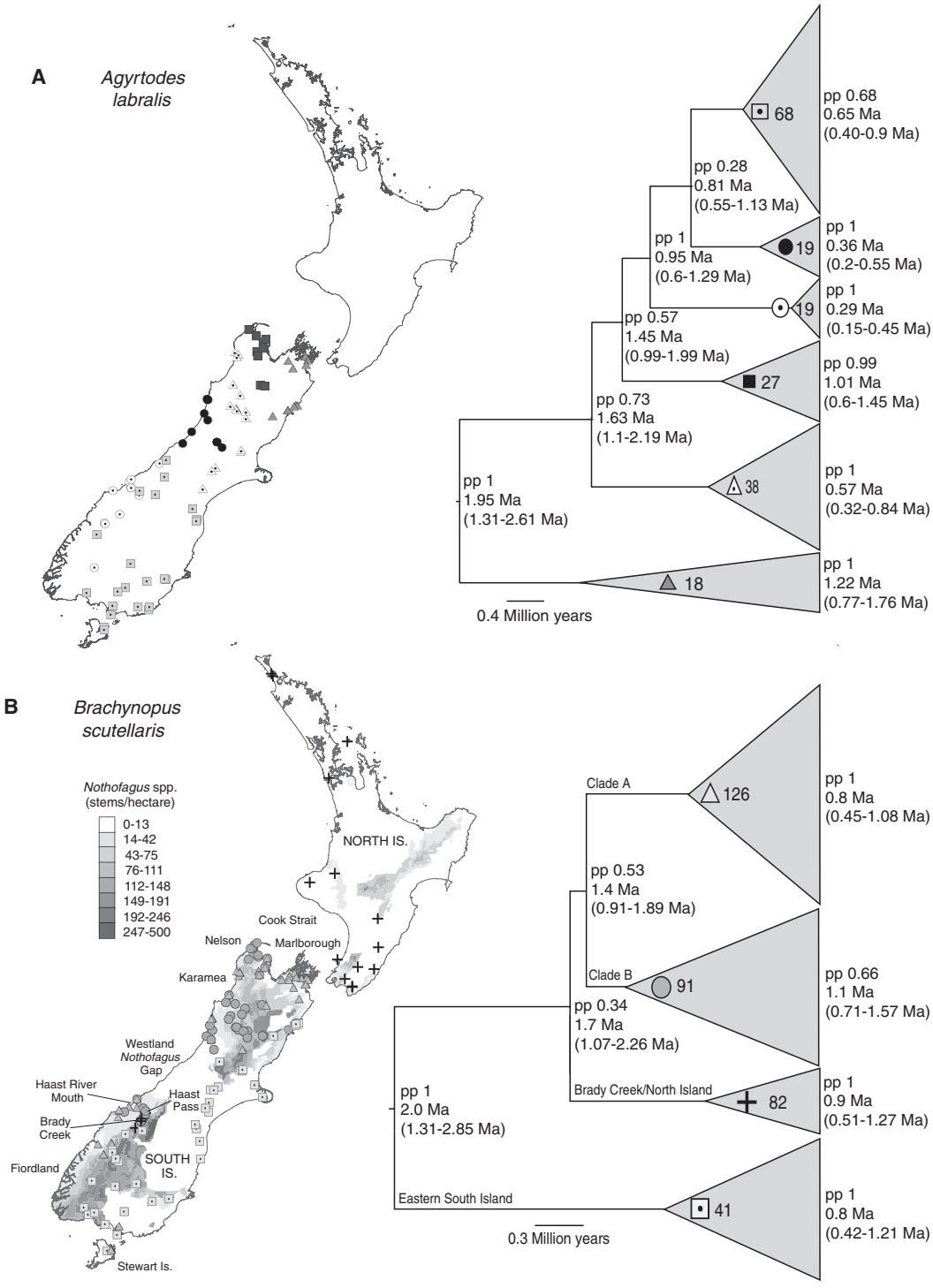

Figure 2. Distributions of (A) *Agyrtodes labralis* and (B) *Brachynopus scutellaris* populations sampled for molecular analysis, and summary of Bayesian coalescent trees with branch lengths drawn proportional to time (millions of years). Clade symbols correspond with map location markers and are next to the number of individuals from each collapsed clade. Map (B) shading indicates the distribution of *Nothofagus* forest (stems/hectare; Leathwick & Austin 2001). Clade labels for *B. scutellaris* follow Leschen *et al.* (2008).

with divergence from the North Island estimated at 5.61 Ma (4.54–6.71 Ma).

Divergences were much shallower for *H. hystrix*, with little support along the backbone of the tree and no well-supported regional haplogroups within the South Island (Fig. 3B). Root coalescence (pp = 1) was between five individuals from Stewart Island and the rest of the tree, estimated at 0.29 Ma (0.15–0.45 Ma). Two North Island clades, comprising northwestern and

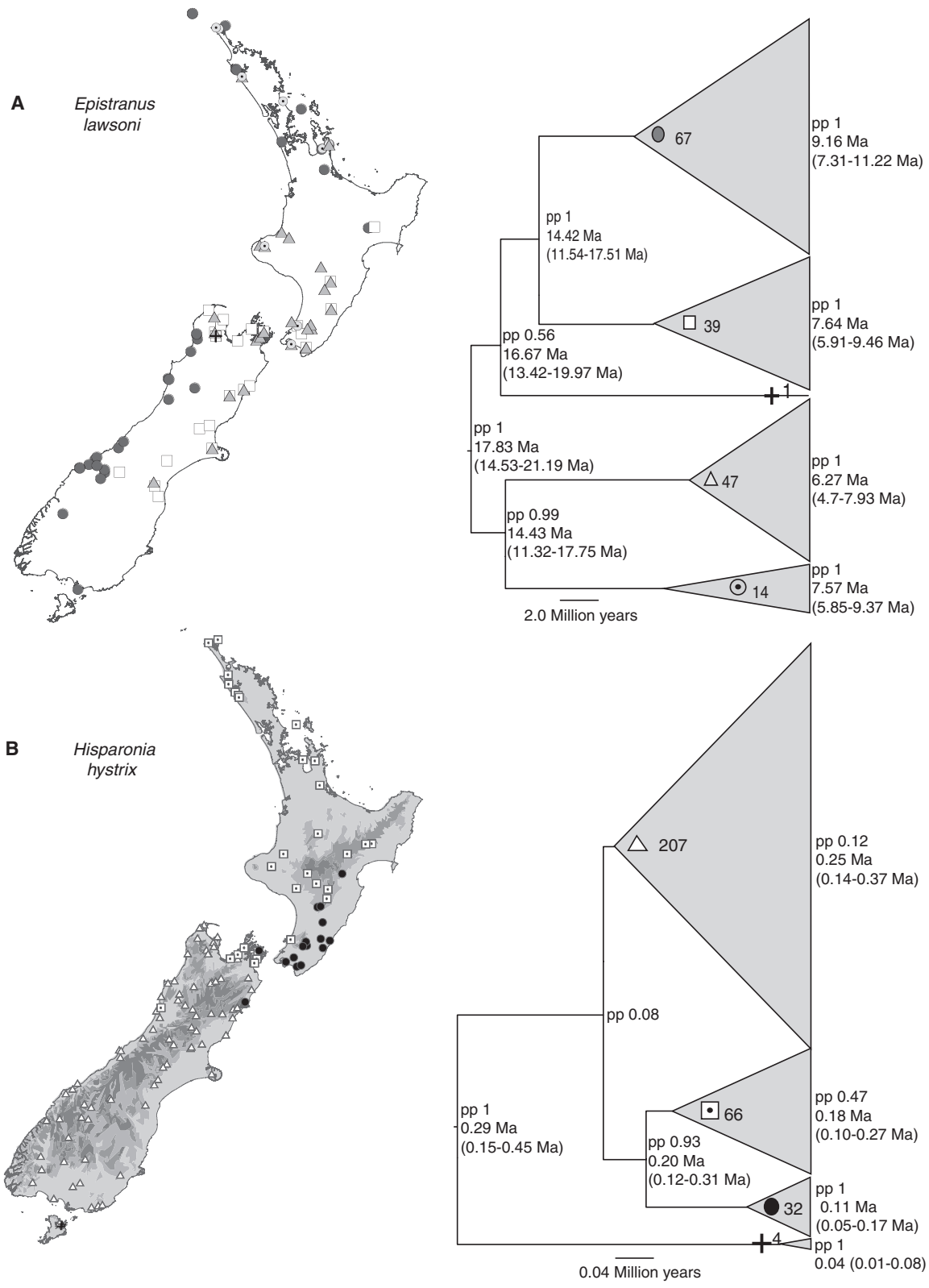

Figure 3. Distributions of (A) *Epistranus lawsoni* and (B) *Hisparonia hystrix* populations sampled for molecular analysis, and summary of Bayesian coalescent trees with branch lengths drawn proportional to time (millions of years). Clade symbols correspond with map location markers and are next to the number of individuals from each collapsed clade. Map (B) shading indicates topographic relief. Note that the *H. hystrix* "clade" indicated by the white triangle is not well-supported.

southeastern lineages, respectively, coalesced at 0.20 Ma (0.12–0.31 Ma, pp = 0.93). Both are also present in the northeastern South Island. Little phylogenetic structure differentiated the remaining South Island lineages.

COALESCENT PHYLOGEOGRAPHIC RECONSTRUCTION

Phylogeographic ancestral state reconstruction for *A. labralis* yielded a scenario slightly different from that outlined in Marske et al. (2009), likely due to the unstable placement of the northern west coast clade (Fig. 2A). Root location was placed in the northern South Island (Kaikoura, state probability, hereafter sp = 0.42; or Nelson–Marlborough, sp = 0.33). The three northern South Island localities were connected first, followed by dispersal to Haast from Nelson via Canterbury, rather than via a west coast route as proposed in Marske et al. (2009) (Fig. 4A). Well-supported rates of geographic state transition for *A. labralis* connected Nelson–Kaikoura, Buller–Canterbury, Canterbury–Haast, Haast–Southland, and Southland–Stewart Island, a subset of the dispersal routes represented in the phylogeny (Table 2; Fig. 5A). All well-supported connections were between neighboring regions, consistent with a stepping-stone dispersal pattern (Lemey et al. 2009).

The matrix of well-supported geographic state transitions relates to the reconstructed dispersal history as follows: Within the MCC tree for *A. labralis*, deep dispersal events connected Kaikoura to Nelson and Nelson to Buller (Fig. 4A, Fig. S2), yet only Kaikoura to Nelson was strongly supported by BSSVS (Table 2, Fig. 5A). The Kaikoura–Nelson transition within the most basal clade was preceded by two nodes where Kaikoura was the best-supported state (sp > 0.7), plus the root (also Kaikoura, sp = 0.42). In contrast, Nelson was relatively weakly supported as the ancestral state (sp = 0.34) at the node giving rise to the Buller–Canterbury clade (Fig. 2A), and the remaining Buller populations, although descended from Nelson, did not have Nelson as their most recent common ancestor (MRCA) (dispersal via Nelson–Canterbury–Haast–Buller, Fig. 4A).

The highest BFs indicated state transitions which occurred multiple times in the MCC tree (e.g., Buller–Canterbury, BF = 33,394.2) and/or where one geographic state was estimated as the only MRCA of another state (e.g., Haast–Southland, BF = 17,809.3), whereas (relatively) lower significant BFs (BF > 3) indicated well-supported but nonexclusive ancestor/descendent relationships (e.g., between Canterbury–Haast, BF = 275.0; Canterbury was both ancestor and descendent of Haast, but Haast was not the only MRCA for Canterbury, which occurred in multiple clades). The matrix of well-supported geographic state transitions is thus an indicator of those dispersal patterns estimated with the greatest confidence throughout the demographic process.

Mapping the phylogeographic history of *B. scutellaris* suggested an early dispersal from the northern South Island to southern North Island (about ~2.5–2 Ma), followed by recent repeated dispersal from the northern to central and southern South Island, largely within the last 0.5 Ma (Fig. 4B). One other dispersal event connected the North (Taranaki) and South (Haast) Islands within the last 0.5 Ma; however, neither interisland event was well-supported by BSSVS, possibly due to ambiguous geographic location of the root state (Nelson, sp = 0.20; Canterbury, sp = 0.14; Haast, sp = 0.14) and low posterior support for the placement of Haast populations within the predominately North Island clade (pp = 0.27). Taranaki, Manawatu, and Northland all had root state probabilities ≤0.05, strongly supporting a South Island origin. Unlike for *A. labralis*, no direct connection was detected between Haast and Canterbury, suggesting that gene flow across the central South Island has been via the coasts rather than across the middle, and dispersal between Buller and Haast was strongly supported, suggesting that opening of the *Nothofagus* gap is too recent (<0.5 Ma) for lineage sorting into distinct halves (Table 2; Fig. 5B). Well-supported geographic state transitions largely represented a subset of the dispersal events captured by the MCC tree; however, Buller–Stewart Island (BF = 4.3) and Taranaki–Northland (BF = 3.8) were well-supported by BSSVS even though neither represented a MRCA relationship.

The dispersal history of *E. lawsoni* largely predated the Pleistocene, with no direct gene flow between the eastern and western South Island throughout the time spanned by the phylogeny. Ancestral state reconstruction using fewer regions than Marske et al. (2011) also identified Northland as the root location (sp = 0.47); all South Island locations had state probabilities ≤0.1 at the root. Three dispersal events originating >4Ma were detected between Northland and the northern South Island, the most recent of which gave rise to the west coast populations (Fig. 4C). However, none of these were strongly supported by BSSVS—likely because increasing the depth of the root (relative to other nodes) increases uncertainty of the root state (Lemey et al. 2009)—leaving Buller–Haast–Southland as an independent network (Table 2; Fig. 5C). Geographic state transitions with BF > 3 comprised a subset of those initiated ≤4Ma and connected neighboring regions, suggesting a recent history of stepping-stone expansion following earlier long-distance dispersal events.

The geographic history of *H. hystrix* was a complex network of recent dispersal events, all within the last 0.5 Ma (Fig. 4D), but low posterior support even for the spine of the MCC tree (Fig. 3B) makes these results difficult to interpret. Nelson received the strongest support as the root location (sp = 0.41), followed by Buller (sp = 0.19); Stewart Island, sister to the rest of the tree, received low support as the ancestral state (sp = 0.03) and is connected to no other regions by BSSVS. Well-supported geographic

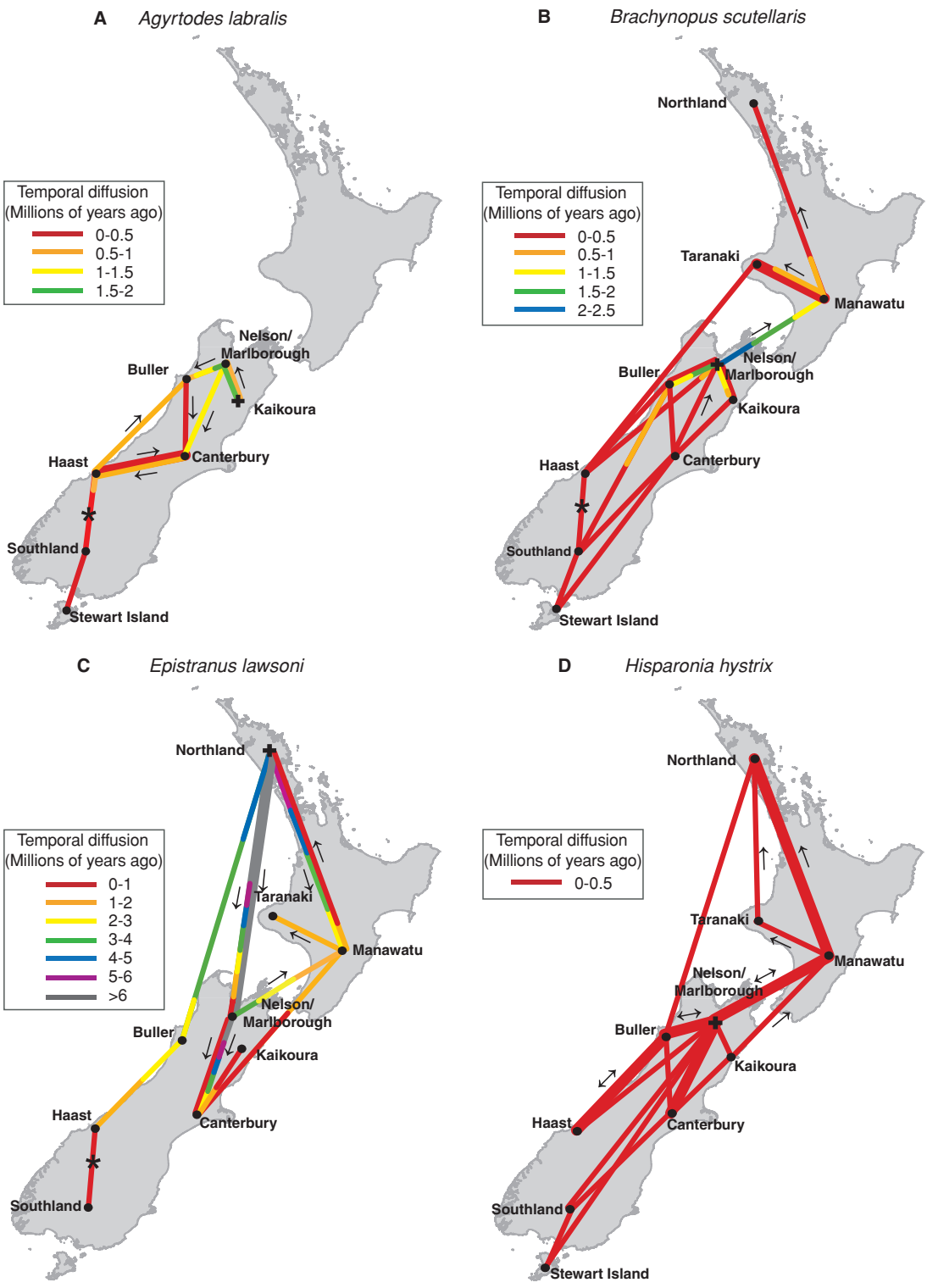

Figure 4. Spatial summary of Bayesian ancestral state reconstruction for (A) *Agyrtodes labralis*, (B) *Brachynopus scutellaris*, (C) *Epistranus lawsoni*, and (D) *Hisparonia hystrix*, rendered for visualization in Google Earth (http://earth.google.com) using code available at the BEAST website. Root location is indicated by a cross. Lines connecting locations indicate branches along which geographic state transitions occur. Note that dispersal is bidirectional between some locations, indicated by double lines. Dispersal is north-south except where indicated by arrows. The transition indicated by * indicates a dispersal pattern shared contemporaneously among the three log-dwelling species but not detected for *H. hystrix*.

Table 2. Bayes factor tests for well-supported (BF>3.0) geographic state transitions. Order of location names does not infer directionality.

Species	Bayes factor	Locations
Agyrtodes labralis	33,394.2	Buller×Canterbury
Agyrtodes labralis	17,809.3	Haast×Southland
Agyrtodes labralis	3256.0	Southland×Stewart Island
Agyrtodes labralis	727.8	Kaikoura×Nelson
Agyrtodes labralis	275.0	Canterbury×Haast
Brachynopus scutellaris	765.8	Manawatu×Taranaki
Brachynopus scutellaris	358.9	Haast×Southland
Brachynopus scutellaris	116.4	Canterbury×Southland
Brachynopus scutellaris	38.9	Canterbury×Kaikoura
Brachynopus scutellaris	38.7	Buller×Canterbury
Brachynopus scutellaris	13.0	Buller×Haast
Brachynopus scutellaris	9.9	Kaikoura×Nelson
Brachynopus scutellaris	6.8	Canterbury×Stewart Island
Brachynopus scutellaris	5.0	Buller×Nelson
Brachynopus scutellaris	4.3	Buller×Stewart Island
Brachynopus scutellaris	4.2	Manawatu×Northland
Brachynopus scutellaris	3.8	Northland×Taranaki
Epistranus lawsoni	15,097.4	Manawatu×Taranaki
Epistranus lawsoni	2320.0	Canterbury×Kaikoura
Epistranus lawsoni	971.1	Haast×Southland
Epistranus lawsoni	36.5	Canterbury×Nelson
Epistranus lawsoni	11.9	Manawatu×Northland
Epistranus lawsoni	8.2	Buller×Haast
Epistranus lawsoni	7.7	Manawatu×Nelson
Hisparonia hystrix	1603.2	Buller×Haast
Hisparonia hystrix	212.6	Buller×Nelson
Hisparonia hystrix	174.9	Manawatu×Taranaki
Hisparonia hystrix	63.1	Canterbury×Kaikoura
Hisparonia hystrix	15.6	Canterbury×Nelson
Hisparonia hystrix	7.8	Manawatu×Northland
Hisparonia hystrix	7.0	Canterbury×Southland
Hisparonia hystrix	4.4	Manawatu×Nelson
Hisparonia hystrix	3.4	Kaikoura×Manawatu

state transitions were largely consistent with a stepping-stone dispersal pattern (Table 2; Fig. 5D).

Discussion

SHARED REFUGIA, DIVERGENT HISTORIES

We proposed three scenarios to explain the response of New Zealand's forest community to Pleistocene glaciation: (1) concurrent spatial and temporal patterns of colonization, suggesting an evolutionary cohort relationship; (2) similar spatial patterns on different time scales, suggesting convergent spatial patterns; and (3) different spatial patterns, suggesting independent evolutionary trajectories. Ecological niche modeling projected broadly congruent spatial histories for *A. labralis*, *B. scutellaris*, and *E. lawsoni* at the LGM (Fig. 1), and Bayesian ancestral state reconstruction with BSSVS identified key geographic connections for each species, facilitating direct temporal comparison of dispersal patterns. In the northern South Island, no well-supported geographic state transitions were shared by more than two of the three log-dwelling species (e.g., Buller–Canterbury, *A. lawsoni* and *B. scutellaris*; Canterbury–Kaikoura, *B. scutellaris* and *E. lawsoni*), and shared dispersal routes were not always concurrent (e.g., Buller–Haast, *B. scutellaris* and *E. lawsoni*) or in the same direction (e.g., Kaikoura–Nelson, *A. labralis* and *B. scutellaris*). However, all three shared a strongly supported dispersal event from Haast–Southland during the last 0.5 Ma. While BSSVS does not attribute geographic state transitions to specific events, differing patterns in the northern South Island likely represent individual responses to the evolving topography, preserved through multiple glacial cycles, while a shared, recent dispersal event in the heavily glaciated south is likely an expansion from a single LGM refugium. Given this combination of concerted versus independent response to glaciation and earlier events, plus evidence for multiple shared glacial refugia, the second scenario (similar spatial patterns on different time scales) better describes the evolutionary relationship among the three log-dwellers, which have repeatedly converged upon similar geographic distributions through a variety of routes.

For the arboreal *H. hystrix*, all geographic state transitions—well-supported or not—occurred <0.5 Ma, and contemporaneous dispersal routes were shared with *B. scutellaris* (Kaikoura–Canterbury, Nelson–Buller–Haast) and *E. lawsoni* (Kaikoura–Canterbury). It is difficult to interpret these results in light of the proposed refugia, as failure of the ENM for *H. hystrix* indicates a niche determined by other factors than the tested climatic variables, such as the distribution of the sooty mould ecosystem, which is in turn driven by the distribution of another insect (Carlton and Leschen 2007). However, phylogenetic results were not qualitatively consistent with refugia hypothesized for the other species, and the only well-supported geographic state transition shared by all three log-dwellers—Haast–Southland—was not detected for *H. hystrix*, suggesting an independent evolutionary trajectory (third scenario).

COALESCENT PHYLOGEOGRAPHY—COMMENDATIONS AND CAVEATS

Statistically rigorous coalescent methods are a vital step toward the fully objective inference of phylogeographic scenarios, particularly in a comparative setting (Knowles 2009; Hickerson et al. 2010). Bayesian coalescent ancestral state reconstruction with BSSVS unites ancestral state reconstruction with statistical phylogeography by inferring the dispersal events across a dated phylogeny while identifying which of those geographic state transitions are best supported by the genetic data. This method has been previously implemented in island/nunatak settings, where the sequence of colonizing events is of interest (Fernández-Mazuecos and Vargas 2011; Lohse et al. 2011); here we introduce it for the

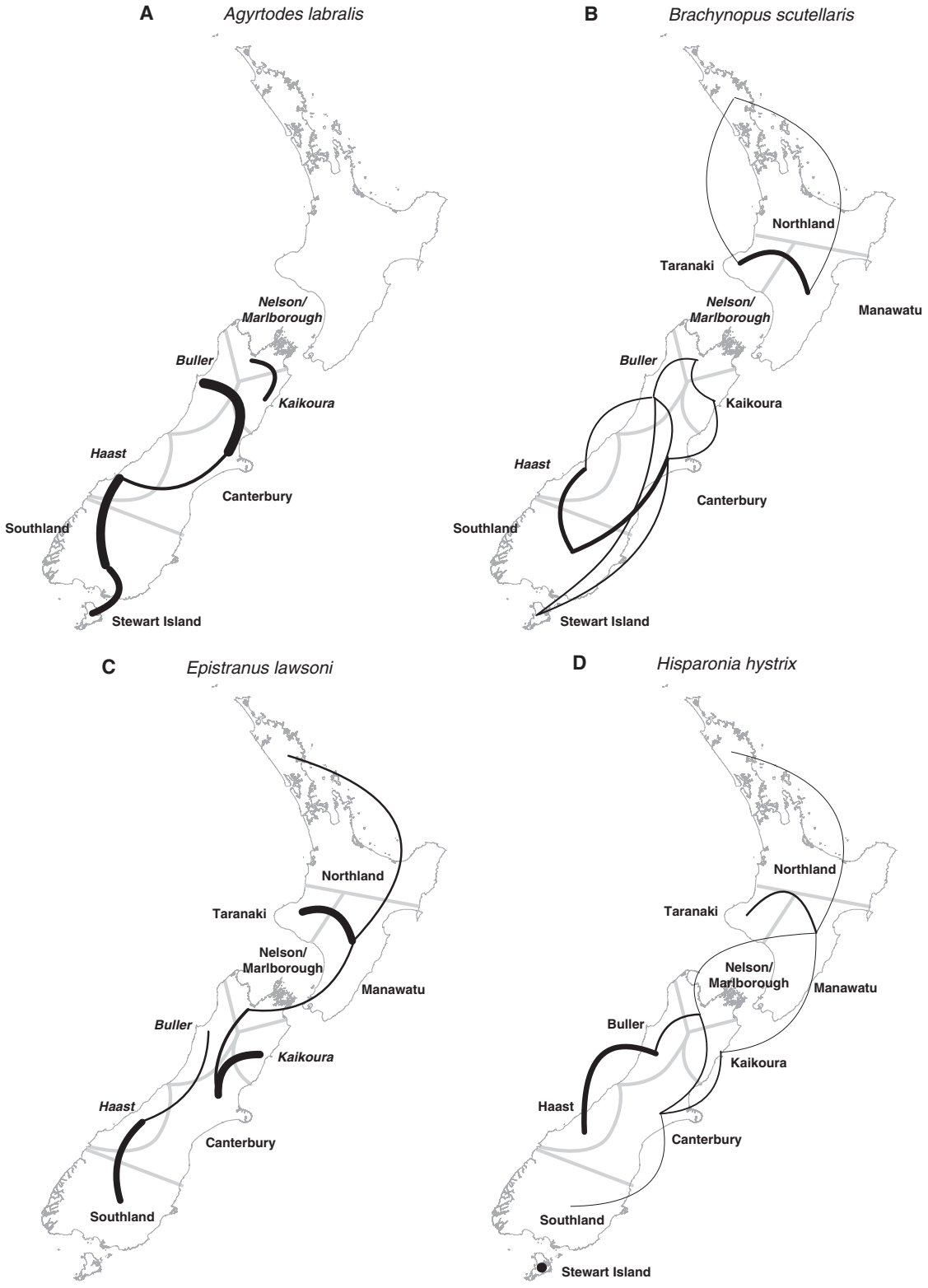

Figure 5. Well-supported (BF > 3.0) geographic state transitions for (A) *Agyrtodes labralis*, (B) *Brachynopus scutellaris*, (C) *Epistranus lawsoni* and (D) *Hisparonia hystrix* identified using Bayesian stochastic search variable selection (BSSVS). Most well-supported transitions are a subset of all geographic state transitions identified in the phylogeny (Figure 4), and thickness of lines indicates the relative strength by which transitions are supported. The shared dispersal event indicated in Figure 4 is strongly supported for the three log-dwelling species, but no other transitions are shared by more than two species. Regions in italics indicate South Island refugia projected for each species by the ENMs.

first time in a comparative setting where BSSVS makes it possible to explicitly identify similarities in the colonization histories of different species.

As implemented here, coalescent ancestral state estimation operates under two geographical assumptions: that the ancestral area is among the localities sampled, and that the spatial diffusion of lineages occurs at a constant rate. Both assumptions may be violated by our data, and how this influences the inference of historic patterns is not obvious (Emerson et al. 2011). Lemey et al. (2010) address the latter issue by relaxing the rate assumption while modeling the spatial diffusion process in continuous, rather than discrete, space. However, this places the ancestral state within the area circumscribed by the sampled localities, whereas in our case, ancestral areas may fall outside of the sampled range. To incorporate our hypothesized refugia as described above, we are therefore restricted to the discrete state method of inference; however, in a dynamic landscape such as New Zealand, identifying a broad region is probably more realistic than trying to pinpoint an ancestral locality. Another disadvantage is that increasing the depth of the root (relative to other nodes) increases geographic uncertainty of the root state and other nodes deep within the phylogeny, but the root location is often less important in phylogeography than divergence within and between clades, particularly here where the root for three of the four species predates the event of interest.

This study was designed to maximize the geographic sampling for each species to increase the chances of detecting glacial refugia, but the trade-off was the use of a single genetic locus. We have previously discussed how reliance on a single locus can affect the precision of coalescent parameter estimates (Marske et al. 2009, 2011). More problematic is that mtDNA may not accurately reflect the genealogical history of a species due to selection or incongruence between gene trees, yielding spurious phylogeographic scenarios. Although Tajima's *D* was nonsignificant for all species, Ilves et al. (2010) highlight the difficulty in differentiating a pattern of rapid colonization following a genetic bottleneck from that of positive selection—either of which would reduce genetic diversity—using a single mitochondrial locus. Although various levels of genetic diversity were detected in the three log-dwelling species, very little was detected for *H. hystrix*, which apparently underwent a recent, rapid dispersal process and for which very little geographic structure was observed in the data. These results are consistent with a severe bottleneck associated with the Pleistocene and LGM, but they are also consistent with a recent selective sweep erasing most mitochondrial diversity within the species, except in the Stewart Island populations. Multi-locus data will be required to infer the history of this species with greater confidence.

Finally, although Bayesian coalescent ancestral state reconstruction with BSSVS is a convenient way to look for similarities in species' spatial histories while accounting for uncertainty in estimating that history, it does not address the underlying processes, particularly here where confidence intervals on dates could include multiple geological events. Explicit population genetics methods, where posterior weight can be placed upon specific events, would be required to address the drivers of observed patterns (e.g., Carstens and Richards 2007; Leaché et al. 2007; Ilves et al. 2010). In this setting, however, different dispersal patterns in the northern South Island are sufficient to indicate different responses to past events; having ruled out the evolutionary cohort hypothesis, explicit identification of particular genetic processes for each species must await further detailed study.

WESTLAND *NOTHOFAGUS* GAP REVISITED

The Westland *Nothofagus* gap features prominently in New Zealand biogeography, both for the mysterious absence of *Nothofagus* (Leathwick 1998) and because the gap phenomenon is repeated in other taxa such as *B. scutellaris*, which shares the central Westland disjunction but is found in the absence of beech in the eastern South Island, Stewart Island, and North Island (Leschen et al. 2008). For *B. scutellaris*, incomplete lineage sorting in two clades straddling the gap (instead of separate northern and southern haplogroups; Figure 2B) and a well-supported geographic state transition <0.5 Ma are consistent with the late Pleistocene gap formation previously inferred with a smaller dataset (Leschen et al. 2008). However, the current projected distribution for *B. scutellaris* indicates that maintenance of this disjunction is not climatically driven, which concurs with similar findings for *Nothofagus* (Leathwick 1998), and *A. labralis* and *E. lawsoni*, which would also have been absent from parts of Westland during the Pleistocene, successfully filled the gap (although projected refugia for these species extended further south, resulting in less gap to fill).

The curious relationship between Buller and Stewart Island in Clade A, in which a well-supported geographic state transition was detected despite a node with an intervening ancestral state, is likely related to the *Nothofagus* gap. Lohse et al. (2011) also observed sister-group populations from neighboring geographic states connected by a well-supported geographic state transition even though neither state was the MRCA of the other, and we observed the same for *B. scutellaris* between Taranaki–Northland, neighboring states. The Buller and Stewart Island populations likely represent a widely-distributed coastal haplogroup sundered at the opening of the gap, which has remained largely undetected south of Haast because of the inaccessibility of coastal Fiordland.

GLACIAL REFUGIA AND FOREST COMMUNITY EVOLUTION

Despite shared LGM refugia and similar modern distributions—suggesting evolutionary trajectories that have repeatedly intersected in space and time—these forest beetles lack the broadly

Table 3. Hypothesized Last Glacial Maximum (LGM) refugia for New Zealand forest invertebrates currently distributed in the South Island which have been sampled throughout their known ranges, from this study and literature descriptions.

Species	Karamea	Nelson/ Marlb.	Haast	Kaikoura	North Island
Agyrtodes labralis	Phy	Phy	Phy	Phy	–
Beetle	ENM	ENM	ENM	ENM	
Brachynopus scutellaris	Phy	Phy	Phy	–	Phy
Beetle	ENM	ENM	ENM		ENM
Epistranus lawsoni					
Beetle	ENM	–	ENM	ENM	ENM
Argosarchus horridus					
Stick insect	–	–	–	Phy	Phy
Buckley et al. 2009				ENM	ENM
Clitarchus hookeri					
Stick insect	–	–	–	–	Phy
Buckley et al. 2010					ENM
Amphipsalta zelandica					
Cicada	ENM	ENM	–	ENM	ENM
Marshall et al., unpubl. ms.					
Kikihia subalpina					
Cicada	Phy	Phy	–	Phy	Phy
Marshall et al. 2009					
Aoraki denticulata		–	–	–	–
Mite harvestman	Phy				
Boyer et al. 2007					

Phy = inferred from phylogenetic data; ENM = identified by ecological niche model; – = inferred absence.

similar population structure which would make them evolutionary cohorts (sensu Carstens and Richards 2007). Our choice of the second proposed phylogeographic scenario (similar spatial patterns on different time scales) for three species has interesting implications for identifying glacial refugia using genetic data. In a multiple refugia scenario, shared refugia do not necessarily result in shared phylogenetic patterns, but different population histories do not negate the possibility of shared refugia—particularly as the mitochondrial history may not reflect the full demographic history of the species. In light of the evidence that biological communities are not necessarily historical entities (e.g., Stewart et al. 2010), it would be interesting to simulate the chances of obtaining cohort-like evolutionary patterns under multiple refugia scenarios, although where multiple refugia are nested within the modern distribution of a species, each additional refugium probably increases the potential dispersal scenarios such that evolutionary cohorts become increasingly less likely. Here detailed dispersal histories for individual species and stochastic lineage sorting issues may obscure actual historical similarities at a broader geographic scale, and the sum of refugia inferred from multiple species may be more instructive about where an ecosystem persisted than looking for shared phylogenetic patterns within an assemblage.

For New Zealand temperate forests, shared refugia among species with strikingly different dispersal histories are a strong indicator of forest survival during the LGM. The sum of dynamics among the log-dwelling beetles, for which we are most confident, suggests that several South Island refugia generated the detected genetic structure. To the Karamea refugium detected by Alloway et al. (2007), ENMs suggest the presence of additional forest refugia at Haast, Nelson/Marlborough, and Kaikoura. Results are broadly consistent for other modeled insect species whose distributions include the South Island: the Kaikoura refugium may have been shared by the stick insect *Argosarchus horridus* (White) (Buckley et al. 2009), and all three northern South Island refugia may have been utilized by the cicada *Amphipsalta zelandica* (Boisduval) (Marshall et al., unpubl. ms.). Other temperate forest invertebrates likely survived in combinations of these refugia (Table 3), and additional studies of comprehensively sampled taxa are expected to yield new insights into their relative importance to New Zealand's forest biota and the roles of concerted versus individual climate response in the recent evolution of ecosystems.

ACKNOWLEDGMENTS

We thank M. Thayer, A. Newton, J. Nunn, J. Allwood, K. Puliafico, L. Clunie, and G. Hall for help with specimens and D. Attanayake, R. Howitt, D. Park, B. Massey, H. Harman, and P. Tsai for laboratory and analytical assistance. G. Barker, C. Briggs, R. Price, F. Morgan, and D. Nogués-Bravo provided advice on ENMs and ArcGIS, and P. Lemey answered questions about the BEAST analysis, which ran at the University of Auckland Bioinformatics Institute and University of Oslo Bioportal. Comments on this manuscript were provided by C. Simon, J. Waters, A. Rodrigo, M. Alfaro and two anonymous referees. Specimens were collected under the Landcare Research Global Concession issued by the Department of Conservation. This research was funded by the Royal Society of New Zealand Marsden Fund (LCR0502) and the Foundation for Research, Science and Technology through the Defining New Zealand's Land Biota OBI, with additional support from the Field Museum of Natural History, the University of Auckland, and the Danish National Research Foundation (to the Center for Macroecology, Evolution and Climate).

LITERATURE CITED

Alloway, B. V., D. J. Lowe, D. J. A. Barrell, R. M. Newnham, P. C. Almond, P. C. Augustinus, N. A. Bertler, L. Carter, N. J. Litchfield, M. S. McGlone, et al. 2007. Towards a climate event stratigraphy for New Zealand over the past 30 000 years (NZ-INTIMATE project). J. Quat. Sci. 22:9–35.

Anderson, R. P., and A. Raza. 2010. The effect of the extent of the study region on GIS models of species geographic distributions and estimates of niche evolution: preliminary tests with montane rodents (genus Nephelomys) in Venezuela. J. Biogeogr. 37:1378–1393.

Bermingham, E., and C. Moritz. 1998. Comparative phylogeography: concepts and applications. Mol. Ecol. 7:367–369.

Boyer, S. L., J. M. Baker, and G. Giribet. 2007. Deep genetic divergences in Aoraki denticulata (Arachnida, Opiliones, Cyphophthalmi): a widespread 'mite harvestman' defies DNA taxonomy. Mol. Ecol. 16:4999–5016.

Brower, A. V. Z. 1994. Rapid morphological radiation and convergence in geographical races of the butterfly, Heliconius erato, inferred from patterns

of mitochondrial DNA evolution. Proc. Natl. Acad. Sci. USA 91:6491–6495.

Buckley, T. R., K. M. Marske, and D. Attanayake. 2009. Identifying glacial refugia in a geographic parthenogen using palaeoclimate modeling and phylogeography: the New Zealand stick insect Argosarchus horridus (White). Mol. Ecol. 18:4650–4663.

———. 2010. Phylogeography and ecological niche modelling of the New Zealand stick insect Clitarchus hookeri (White) support survival in multiple coastal refugia. J. Biogeogr. 37:682–695.

Carlton, C., and R. A. B. Leschen. 2007. Descriptions of Soronia complex (Coleoptera: Nitidulidae: Nitidulinae) larvae of New Zealand with comments on life history and taxonomy. N. Z. Entomol. 30:41–51.

Carstens, B. C., S. J. Brunsfeld, J. R. Demboski, J. D. Good, and J. Sullivan. 2005. Investigating the evolutionary history of the Pacific Northwest mesic forest ecosystem: hypothesis testing within a comparative phylogeographic framework. Evolution 59:1639–1652.

Carstens, B. C., and C. L. Richards. 2007. Integrating coalescent and ecological niche modeling in comparative phylogeography. Evolution 61:1439–1454.

Drummond, A. J., and A. Rambaut. 2007. BEAST: Bayesian evolutionary analysis by sampling trees. BMC Evol. Bio. 7:214.

Emerson, B. C., F. Cicconardi, P. P. Fanciulli, and P. J. A. Shaw. 2011. Phylogeny, phylogeography, phylobetadiversity and the molecular analysis of biological communities. Philos. Trans. R. Soc. B 366:2391–2402.

Fernández-Mazuecos, M., and P. Vargas. 2011. Genetically depauperate in the continent but rich in oceanic islands: Cistus monspeliensis (Cistaceae) in the Canary Islands. PLoS One 6:e17172.

Hall, T. A. 1999. BioEdit: a user-friendly biological sequence alignment editor and analysis program for Windows 95/98/NT. Nucleic Acids Symp. Ser. 41:95–98.

Hewitt, G. 2000. The genetic legacy of the Quaternary ice ages. Nature 405:907–913.

Hickerson, M.J., B. C. Carstens, J. Cavender-Bares, K. A. Crandall, C. H. Graham, J. B. Johnson, L. Risslerf, P. F. Victoriano, and A. D. Yoder. 2010. Phylogeography's past, present, and future: 10 years after Avise, 2000. Mol. Phylogenet. Evol. 54:291–301.

Ilves, K. L., W. Huang, J. P. Wares, and M. J. Hickerson. Colonization and/or mitochondrial selective sweeps across the North American intertidal assemblage revealed by multi-taxa approximate Bayesian computation. Mol. Ecol. 19:4505–4519.

King, P. R. 2000. Tectonic reconstructions of New Zealand: 40 Ma to the present. N. Z. J. Geol. Geophys. 43:611–638.

Knowles, L. L. 2009. Statistical phylogeography. Ann. Rev. Ecol. Evol. Syst. 40:593–612.

Leaché, A., S. A. Crews, and M. J. Hickerson. 2007. Did an ancient seaway across Baja California cause community isolation? Biol. Lett. 3:646–650.

Leathwick, J., F. Morgan, G. Wilson, D. Rutledge, M. McLeod, K. Johnston. 2003. Land Environments of New Zealand: a Technical Guide. David Bateman, Auckland, New Zealand.

Leathwick, J. R. 1998. Are New Zealand's Nothofagus species in equilibrium with their environment? J. Veg. Sci. 9:719–732.

———. 2001. New Zealand's potential forest pattern as predicted from current species: environment relationships. N. Z. J. Bot. 39:447–464.

Leathwick, J. R., and M. P. Austin. 2001. Competitive interactions between tree species in New Zealand's old-growth indigenous forests. Ecology 82:2560–2573.

Leathwick, J. R., G. Wilson, and R. T. T. Stephens. 1998. Climate surfaces for New Zealand. Landcare Research Contract Report LC9798/ 126. Landcare Research, Hamilton.

Lemey, P., A. Rambaut, A. J. Drummond, and M. A. Suchard. 2009. Bayesian phylogeography finds its roots. PLoS Comput. Biol. 5:e1000520.

Lemey, P., A. Rambaut, J. J. Welch, and M. A. Suchard. 2010. Phylogeography takes a relaxed random walk in continuous space and time. Mol. Biol. Evol. 27:1877–1885.

Leschen, R. A. B., T. R. Buckley, H. M. Harman, and J. Shulmeister. 2008. Determining the origin and age of the Westland Beech (Nothofagus) gap, New Zealand, using fungus beetle genetics. Mol. Ecol. 17: 1256–1276.

Löbl, I., and R. A. B. Leschen. 2003. Scaphidiinae (Insecta: Coleoptera: Staphylinidae). Fauna of New Zealand No. 48, Manaaki Whenua Press, Lincoln, Canterbury, New Zealand. 94 pp.

Lohse, K., J. A. Nicholls, and G. N. Stone. 2011. Inferring the colonization of a mountain range—refugia vs. nunatak survival in high alpine ground beetles. Mol. Ecol. 20:394–408.

Marra, M. J., and G. D. Thackray. 2010. Glacial forest refugium in Howard Valley, South Island, New Zealand. J. Quat. Sci. 25:309–319.

Marshall, D. C., K. B. R. Hill, T. R. Buckley, K. Fontaine, and C. Simon. 2009. Glacial refugia in a maritime temperate climate: cicada (Kikihia subalpina) mtDNA phylogeography in New Zealand. Mol. Ecol. 18:1995–2009.

Marske, K. A., R. A. B. Leschen, G. M. Barker, and T. R. Buckley. 2009. Phylogeography and ecological niche modeling implicate coastal refugia and trans-alpine dispersal of a New Zealand fungus beetle. Mol. Ecol. 18:5126–5142.

Marske, K. A., R. A. B. Leschen, and T. R. Buckley, 2011. Reconciling phylogeography and ecological niche models for New Zealand beetles: Looking beyond glacial refugia. Mol. Phylogenet. Evol. 59: 89–102.

McCormack, J. E., A. J. Zellmer, and L. L. Knowles, 2010. Does niche divergence accompany allopatric divergence in Aphelocoma jays as predicted under ecological speciation? Insights from tests with niche models. Evolution 64:1231–1244.

McGlone, M. S. 1985. Plant biogeography and the late Cenozoic history of New Zealand. N. Z. J. Bot. 23:723–749.

McGovern, T. M., C. C. Keever, C. A. Saski, M. W. Hart, and P. B. Marko, 2010. Divergence genetics analysis reveals historical population genetic processes leading to contrasting phylogeographic patterns in co-distributed species. Mol. Ecol. 19:5043–5060.

Papadopoulou, A., I. Anastasiou, and A. P. Vogler. 2010. Revisiting the insect mitochondrial molecular clock: the Mid-Aegean Trench calibration. Mol. Biol. Evol. 27:1659–1672.

Pearce, J., and S. Ferrier. 2000. Evaluating the predictive performance of habitat models developed using logistic regression. Ecol. Model. 133:225–245.

Pearson, R. G., C. J. Raxworthy, M. Nakamura, and A. T. Peterson, 2007. Predicting species distributions from small numbers of occurrence records: a test case using cryptic geckos in Madagascar. J. Biogeogr. 34: 102–117.

Phillips, S. J., and Dudík, M. 2008. Modeling of species distributions with Maxent: new extensions and a comprehensive evaluation. Ecography 31:161–175.

Phillips, S. J., R. P. Anderson, and R. E. Schapire, 2006. Maximum entropy modelling of species geographic distributions. Ecol. Model. 190:231–259.

Phillips, S. J., M. Dudík, J. Elith, C. H. Graham, A. Lehmann, J. Leathwick, and S. Ferrier. 2009. Sample selection bias and presence-only distribution models: implications for background and pseudo-absence data. Ecol. Appl. 19:181–197.

Posada, D., and K. A. Crandall. 1998. Modeltest: testing the model of DNA substitution. Bioinformatics 14:817–818.

Pulford, A., and T. Stern. 2004. Pliocene exhumation and landscape evolution of central North Island, New Zealand: the role of the upper mantle. J. Geophys. Res. 109:F01016.

Raes, N., and H. ter Steege. 2007. A null-model for significance testing of presence-only species distribution models. Ecography 30:727–736.

Rambaut, A., and A. J. Drummond. 2009. Tracer v1.5. Available at: http://beast.bio.ed.ac.uk/Tracer (accessed December 29, 2009).

Rozas, J., J. C. Sánchez-DelBarrio, X. Messeguer, and R. Rozas. 2003. DnaSP: DNA polymorphism analyses by the coalescent and other methods. Bioinformatics 19:2496–2497.

Seago, A. E. 2009. Revision of Agyrtodes Portevin (Coleoptera: Leiodidae). The Coleopterists Society Monographs 7:1–73.

Shepherd, L. D., and L. R. Perrie. 2011. Microsatellite DNA analyses of a highly disjunct New Zealand tree reveal strong differentiation and imply a formerly more continuous distribution. Mol. Ecol. 20:1389–1400.

Shepherd, L. D., L. R. Perrie, and P. J. Brownsey. 2007. Fire and ice: volcanic and glacial impacts on the phylogeography of the New Zealand forest fern Asplenium hookerianum. Mol. Ecol. 16:4536–4549.

Simon, C., F. Frati, B. Crespi, H. Liu, and P. K. Flook. 1994. Evolution, weighting, and phylogenetic utility of mitochondrial gene sequences and a compilation of conserved PCR primers. Ann. Entomol. Soc. Am. 87:651–701.

Soltis, D. E., A. B. Morris, J. S. McLachlan, P. S. Manos, and P. S. Soltis. 2006. Comparative phylogeography of unglaciated eastern North America. Mol. Ecol. 15:4261–4293.

Stewart, J. R., A. M. Lister, I. Barnes, and L. Dalén. 2010. Refugia revisited: individualistic responses of species in space and time. Proc. R. Soc. Lond. B 277:661–671.

Suggate, R. P., and P. C. Almond, 2005. The Last Glacial Maximum (LGM) in western South Island, New Zealand: implications for the global LGM and MIS 2. Quat Sci. Rev. 24:1923–1940.

Sullivan, J., E. A. Arellano, and D. S. Rogers. 2000. Comparative phylogeography of Mesoamerican highland rodents: concerted versus independent responses to past climatic fluctuations. Am. Nat. 155:755–768.

Swofford, D. L. 1998. PAUP*. Phylogenetic analysis using parsimony (*and other methods), Version 4. Sinauer Associates, Sunderland, MA.

Veloz, S. D. 2009. Spatially autocorrelated sampling falsely inflates measures of accuracy for presence-only niche models. J. Biogeogr. 36:2290–2299.

Waltari, E., R. J. Hijmans, A. T. Peterson, Á. Nyári, S. Perkins, and R. P. Guralnick. 2007. Locating Pleistocene refugia: comparing phylogeography and ecological niche model predictions. PLoS One 7:e563.

Associate Editor: M. Alfaro

Supporting Information

The following supporting information is available for this article:

Appendix S1: Input localities for ENMs, detailed phylogenies for all four species, and collection localities for *Brachynopus scutellaris* and *Hisparonia hystrix*.
Figure S1. Input localities for ENMs for each species.
Figure S2. Map and Bayesian coalescent tree for *Agyrtodes labralis*.
Figure S3. Map and Bayesian coalescent tree for *Brachynopus scutellaris*.
Figure S4. Map and Bayesian coalescent tree for *Epistranus lawsoni*.
Figure S5. Map and Bayesian coalescent tree for *Hisparonia hystrix*.
Table S1. Collection localities for newly sequenced individuals of *Agyrtodes labralis*.
Table S2. Collection localities for all sequenced individuals of *Brachynopus scutellaris*.
Table S3. Collection localities for all sequenced individuals of *Hisparonia hystrix*.

Supporting Information may be found in the online version of this article.

Please note: Wiley-Blackwell is not responsible for the content or functionality of any supporting information supplied by the authors. Any queries (other than missing material) should be directed to the corresponding author for the article.